JCTC Journal of Chemical Theory and Computation

Article

pubs.acs.org/JCTC

Assessment of a Cost-Effective Approach to the Calculation of Kinetic and Thermodynamic Properties of Methyl Methacrylate Homopolymerization: A Comprehensive Theoretical Study

Guozhen Zhang,[†] Ivan A. Konstantinov,[‡] Steven G. Arturo,[§] Decai Yu,[∥] and Linda J. Broadbelt*[,†]

[†]Department of Chemical and Biological Engineering, Northwestern University, Evanston, Illinois 60208, United States

[‡]The Dow Chemical Company, 2301 N. Brazosport Blvd., Freeport, Texas 77541, United States

[§]The Dow Chemical Company, 400 Arcola Rd., Collegeville, Pennsylvania 19426, United States

[∥]The Dow Chemical Company, 1776 Building, Midland, Michigan 48674, United States

Supporting Information

ABSTRACT: In this work, we carried out a comprehensive density functional theory (DFT) study on the basis of a trimer-to-tetramer radical reaction model to assess a cost-effective approach to perform the calculation of kinetic and thermodynamic properties of methyl methacrylate (MMA) free-radical homopolymerization. By comparing results from several different functionals (PBE, M06-2X, wB97XD, KMLYP, and MPW1B95), in conjunction with a series of basis sets (6-31G(d,p), 6-31+G(d,p), 6-31G(2df,p), 6-311G(d,p), 6-311+G(d,p), 6-311+G(2df,p), 6-311+G(2df,2p)), we show that calculations using M06-2X/6-311+G(2df,p)//B3LYP/6-31G(2df,p) provide an activation energy of 5.25 kcal mol^{-1} for the homopropagation step, which is within 1 kcal mol^{-1} of the experimental value. However, this method predicts a heat of polymerization of 17.37 kcal mol^{-1} that is larger than the experimental value by 3.5 kcal mol^{-1}. MPW1B95/6-311+G(2df,p) on the B3LYP/6-31G(2df,p) geometries produces a heat of polymerization value within 1 kcal mol^{-1} of experimental data, yet overestimates the activation energy by 3 kcal mol^{-1}. In addition, we evaluated the performance of ONIOM MO:MO calculations on the geometry optimization of species comprising our MMA polymerization model and found that ONIOM(B3LYP/6-31G(2df,p):B3LYP/6-31G(d)) is capable of producing geometries in very good agreement with the full B3LYP/6-31G(2df,p) calculations. Subsequent calculations of energies using M06-2X/6-311+G(2df,p) based on the ONIOM geometries provided an activation energy value comparable to that based on the full B3LYP/6-31G(2df,p) geometries.

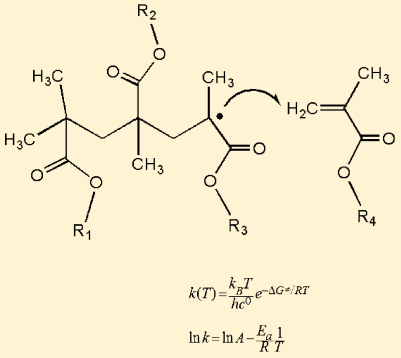

$$k(T)=\frac{k_B T}{hc^0}e^{-\Delta G^{\neq}/RT}$$

$$\ln k=\ln A-\frac{E_a}{R}\frac{1}{T}$$

1. INTRODUCTION

Methyl methacrylate (MMA) is used to prepare a wide range of polymeric materials, such as resins and plastics. These materials have many important industrial applications, including displays, lighting panels, durable coatings, and inks.[1] Free-radical chain polymerization, comprised of initiation, propagation, and termination steps, is the main approach to produce acrylic polymers.[2] The propagation rate plays a significant role in determining molecular weight (MW), molecular weight distribution (MWD), and composition for co-polymers, all of which are associated with the performance of products.[3] Therefore, accurate measurement of the propagation rate is critical in controlling radical polymerization to make the desired products. Since the late 1980s, pulsed laser polymerization, in conjunction with size exclusion chromatography (PLP-SEC), has been developed and has become a standard technique for measuring free-radical propagation rate coefficients.[3] It has been applied to obtain reliable propagation rate coefficients for various acrylate polymers in bulk and in solution.[3] However, some recipes for acrylate-based materials can contain multiple bulky monomers,[4,5] and cross-propagation rate coefficients, including a wide diversity of possible penultimate or higher order effects, are needed to quantitatively describe the system.[6,7] Therefore, it is desirable to have theoretical methods that can be used as a complement to experimental measurements to predict all possible rate coefficients accurately. Quantum chemistry calculations have been increasingly used as an alternative approach to support and to enrich experimental studies of polymeric reactions.[8−23] They are able to provide kinetics information for each possible combination of monomers and penultimate effects to establish structure−reactivity relationships.[8,19,22] The calculated propagation rate coefficients can be used selectively for modeling polymerization processes to gather useful information about MWD and chain sequences.[24−26] The structure−reactivity relationships can facilitate screening of monomers for the design of new polymers with targeted properties, and they can be extended to systems of monomers beyond those employed to develop the structure−reactivity relationships.

There has been a growing body of research on calculating propagation coefficients of acrylate polymers using quantum

Received: June 10, 2014

   dx.doi.org/10.1021/ct500507f | J. Chem. Theory Comput. XXXX, XXX, XXX−XXX

chemistry calculations in the past decade. Yu et al. conducted a comprehensive study on MMA and methyl acrylate (MA) and evaluated effects from low frequency internal motions, chain length of the mimic of the polymer chain used for calculation, and solvent. They concluded that low-frequency modes treated by a one-dimensional hindered rotor (1D-HR) model can give better estimates of the propagation rate coefficients than a harmonic oscillator (HO) model does. However, since the effect of the low-frequency modes is not significant for the activation energy values, using the HO model can provide activation energy results comparable to those obtained using an HR model.[11,12,23] In addition, solvent effects treated by an implicit solvent model play an insignificant role in determining activation energy, as long as the solvent polarity is not significant.[12] Değirmenci et al. investigated the effect of pendant groups on the polymerizability of various acrylates and methacrylates.[19] They also studied the tacticity in the free-radical polymerization of several α-substituted acrylates (including MMA) and reproduced the dominance of syndiotacticity in the case of MMA that has been found by experiment.[20] The same work also examined solvent effects on the tacticity of MMA polymerization using explicit solvent molecules, as well as a polarizable dielectric continuum model, showing that alcohol solvents can restrain the formation of isotactic structures when there exists hydrogen bonding between solute and solvent molecules.[21] Miller and Holder studied structure−activity relationships in the homopolymerization of methacrylates and found that the electronic effect of radicals could be responsible for large propagation rate coefficients of large methacrylate monomers.[22] Yavuz and Çiftçioğlu benchmarked the performance of various functionals using density functional theory (DFT) in the complete basis set (CBS) limit on the first step of MA polymerization. They found that MPW1B95, M06-2X, and wB97XD performed well in the calculation of activation energy values in the CBS limit, and the values in this limit are systematically ∼20% larger than those calculated with the cc-PVTZ basis set. They also found that the use of a 1D-HR model effectively improves the theoretical prediction of rate coefficients.[23]

Although these previous quantum chemistry studies on acrylate polymers provide useful information about factors (e.g., solvent effect, penultimate effect, and internal rotation of a molecule) relevant to propagation, they shed little light on the quantification of a cost-effective approach for the study of acrylate polymerization. For example, most of these works carried out DFT calculations and did not provide a clear answer what combination of functional and basis set was best for acrylates. The work of Yavuz and Çiftçioğlu comes the closest in this regard, in which MA polymerization was studied,[23] but they did not examine penultimate effects. On the other hand, Lin et al. have argued that DFT calculations of the propagation rate coefficient of MA are unreliable, in comparison with high level G3(MP2)-RAD calculations.[14] However, the reaction barrier for the monomer-to-dimer model of MA at the G3(MP2)-RAD level of accuracy was reported to be 1.2 kcal mol^{-1}.[10,14] This value is too low, relative to the experimental value (4.2 kcal mol^{-1}).[27] The lack of consensus on what computational method should be used raises a critical question: What is a cost-effective approach for the study of MMA polymerization and other methacrylate polymerization?

To identify a viable recipe for the theoretical study of reaction kinetics of polymerization of MMA and other acrylates, we carried out a benchmark test of DFT methods with a particular focus on newly developed functionals and different basis sets in this work. We also investigated the feasibility of speeding up geometry optimizations using the ONIOM[28] method. We utilized the trimer-to-tetramer radical model, which can capture penultimate effects for future studies of co-polymerization with one unit included beyond the penultimate unit and also to maximize computational efficiency while still obtaining accurate results. Because one could vary the size of the reacting system while also changing the basis set and functional to match properties of interest, our trimer-to-tetramer radical model is not a unique choice to model polymerization systems. However, it is a reasonable choice that has been shown to adequately describe the rate coefficients of both MA and MMA propagation by a previous study.[12]

2. COMPUTATIONAL METHODS

All calculations were carried out using the Gaussian 09 program.[29] Various DFT methods have been employed in this work, coupled with basis sets of different sizes. The variation of results using different methods for geometry optimization was explored, and energies were then calculated at different levels of theory to evaluate their ability to capture activation energy (E_a) and heat of polymerization (ΔH_p) values.

For geometry optimization, we employed the B3LYP[30] functional, coupled with the 6-31G(2df,p) basis set. It is noted that this level of theory was also adopted in the Gaussian-4(G4) method,[31] the latest generation of an accurate composite approach for computing energies. On the basis of optimized structures, vibrational frequencies based on the harmonic oscillator approximation were then calculated to obtain zero-point energies (ZPEs) and free energies using standard formulas from statistical mechanics.[32] A scale factor of 0.9854 was applied to the obtained frequencies to mitigate known deficiencies of unscaled frequencies.[31] Reactants and products along the reaction coordinate were confirmed to be minima with no imaginary frequencies, and transition states (TS) were confirmed to be first-order saddle points on the potential energy surface (PES), characterized by one imaginary frequency. A TS was then validated by an intrinsic reaction coordinate (IRC) calculation.[33]

Since locating optimized structures was typically the most time-consuming part of our computations, we then applied the ONIOM method[28] to perform geometry optimization, with the objective of speeding up the calculations without significantly sacrificing the accuracy of results. ONIOM divides a large system into two or three layers, on the basis of the relevance of each layer to the chemistry being studied, and treats them at different levels of theory. In this work, we applied a two-layer ONIOM model to all species involved, so that the region highly related to the formation of the new carbon−carbon bond was allocated to the high-level layer and the surrounding region was allocated to the low-level layer. In the ONIOM method, the entire molecule (i.e., the combination of the high-level layer and the low-level layer) is also known as the real system (RS). When the low-level layer is effectively reduced to a link atom (typically a hydrogen atom), the real system becomes the model system (MS). The energy of a system treated by the ONIOM approach is calculated using eq 1:

$$E^{\mathrm{ONIOM}} = E^{\mathrm{low}}(\mathrm{RS}) + E^{\mathrm{high}}(\mathrm{MS}) - E^{\mathrm{low}}(\mathrm{MS}) \quad (1)$$

In eq 1, "high" and "low" refer to high and low levels of theory, respectively. The advantage of the ONIOM method lies in flexible combinations of different methods applied to different layers. When two levels of electronic structure methods are employed in an ONIOM calculation, it is referred to as an MO:MO calculation. [Note that "MO" denotes molecular orbital.] In this work, we carried out MO:MO calculations, in which B3LYP/6-31G(2df,p) was employed for the MS, and B3LYP coupled with different smaller basis sets (including 6-31G(d), 6-31G(d,p), and 6-31+G(d,p)) was used for the RS.

dx.doi.org/10.1021/ct500507f | J. Chem. Theory Comput. XXXX, XXX, XXX−XXX

The important aspect of the ONIOM calculations is the assignment of the model system, which partitions the system into a high-level layer and a low-level layer. We tested three different model systems generated from three different ONIOM partition schemes, depicted in Figure 1. In partition 1, the methyl group in each ester moiety is part of the low-level layer. This is based on the assumption that these methyl groups have a negligible impact on the geometry of the reaction center in the TS. In partition 2, the two repeating units furthest from the radical center are assigned to the low-level layer. This partition is consistent with an earlier theoretical work by Izgorodina and Coote on the study of acrylonitrile and vinyl chloride[11] and seems reasonable based on treating the two monomer units furthest away from the reactive center at a lower level of theory. Partition 3 is similar to partition 2 but also includes the methyl groups on ester moieties of all units in the low-level layer. For each partition scheme, three sets of MO:MO calculations were carried out using B3LYP/6-31G(2df,p):B3LYP/6-31G(d), B3LYP/6-31G(2df,p):B3LYP/6-31G(d,p), and B3LYP/6-31G(2df,p):B3LYP/6-31+G(d,p), respectively.

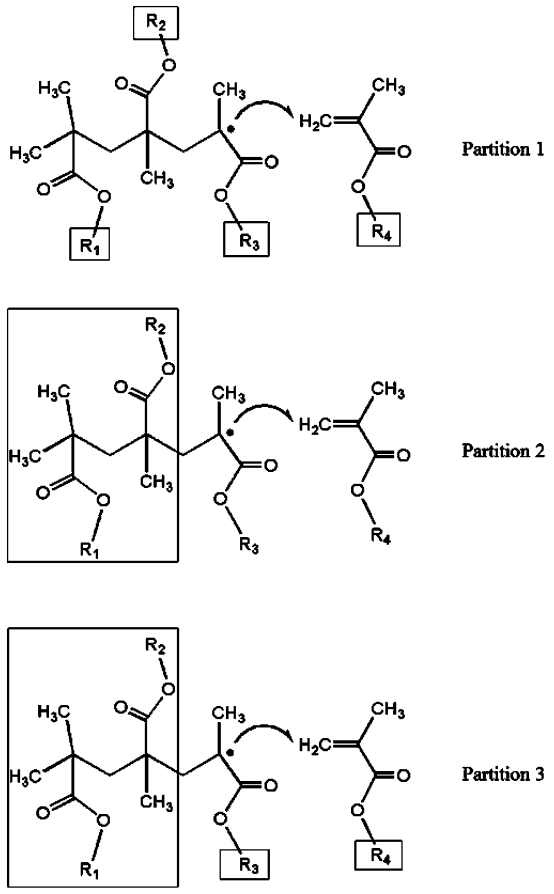

Figure 1. Representations of three different ONIOM partitioning schemes. Boxed regions are treated as low-level layers in ONIOM calculations.

After locating all designated species on the reaction coordinate, we conducted a series of single-point calculations to compute the activation energy and heat of polymerization of MMA homopolymerization. Specifically, we did a two-dimensional search to identify an optimal combination of DFT functional and basis set. Regarding DFT functionals, we employed PBE,[34] KMLYP,[35] MPW1B95,[36] M06-2X,[37] and wB97XD.[38] These functionals are representatives of different types of DFT methods. PBE is regarded as a representative example of nonempirical pure functionals using the generalized gradient approximation (GGA).[39] It is thus valuable for any benchmark work of DFT methods on molecular systems. KMLYP is a hybrid functional designed for accurate prediction of reaction barriers.[35] Both MPW1B95 and M06-2X are hybrid meta-GGAs optimized for general applications of thermochemistry, kinetics, and noncovalent interactions.[36,37] wB97XD is a long-range corrected (LC) hybrid functional incorporating additional empirical dispersion corrections that has been reported to do reasonably well in predicting thermochemistry, kinetics, and noncovalent interactions.[38] Moreover, most of these DFT methods have been reported to perform well in theoretical studies of radical polymerization systems. Izgorodina and Coote have reported that KMLYP and MPW1B95 perform well for homopolymerization of acrylonitrile and vinyl chloride.[11] Yavuz and Çiftçioğlu have reported that M06-2X and wB97XD capture the homopolymerization of methyl acrylate well.[23] For basis sets, we considered 6-31G(d,p), 6-31+G(d,p), 6-31G(2df,p), 6-311G(d,p), 6-311+G(d,p), 6-311+G(2df,p), and 6-311+G(2df,2p). For C, H, and O atoms, 6-311+G(2df,2p) is equivalent to Truhlar's MG3 semidiffuse (MG3S) basis set.[40] Because of the incompleteness of a finite size basis set, the basis set superposition error (BSSE) pertains to combination reaction systems (i.e., A + B → C), such as those studied here.[41] Thus, a correction using the counterpoise method was applied to the uncorrected results in order to take BSSE into account.[42]

Details of how to calculate activation energy and pre-exponential factor (A) values, using thermochemistry data from quantum chemistry calculations, can be found elsewhere.[21,43] Briefly, E_a and A are calculated using the Arrhenius equation, in conjunction with transition state theory (TST). In TST, reactants (R), the transition state (TS), and products (P) are identified along the reaction coordinate, and the rate coefficient, $k(T)$, is computed according to eq 2:

$$k(T) = \sigma\left(\frac{k_B T}{h}\right)(c^0)^{1-m}\exp\left(-\frac{\Delta G^{\ddagger}}{RT}\right) \quad (2)$$

where σ is the reaction path degeneracy, k_B is Boltzmann's constant (1.38×10^{-23} J mol^{-1} K^{-1}), T is the absolute temperature (K), h is Planck's constant (6.626×10^{-34} J s), R is the universal gas constant (8.314 J mol^{-1} K^{-1}), c^0 is a pressure- and temperature-dependent concentration factor used to account for the standard state, m is the number of reactants, and $\Delta G^{\ddagger}$ is the free-energy difference between TS and reactants for the forward reaction or between TS and products for the reverse reaction. Given a set of $k(T)$ values calculated at a series of T, E_a and A are obtained through linear regression following eq 3:

$$\ln k(T) = \ln A - \left(\frac{E_a}{R}\right)\left(\frac{1}{T}\right) \quad (3)$$

In this work, the temperature range used for calculation of the activation energy was −40 °C to 120 °C, covering the common temperature range over which PMMA is synthesized in experiments.[44]

3. RESULTS AND DISCUSSION

In section 3.1, we apply DFT to explore conformational space of the structures used in this study to identify the lowest energy conformers. In section 3.2, we use these conformers to test a variety of functionals for the calculation of kinetic and thermodynamic properties. In section 3.3, we explored different ONIOM partition schemes and different combinations of methods for MO:MO calculations in order to determine a cost-effective approach to carry out geometry optimizations for MMA polymerization and potentially larger acrylate-based polymers.

3.1. Identification of Low-Energy Conformations of Structures. The MMA monomer can adopt two different conformations based on the relationship of the alkene moiety and the carbonyl moiety. As shown in Figure 2, they can be arranged either in a *cis* pattern, for which the conformer is termed as *s-cis*, or in a *trans* pattern, for which the conformer is termed as *s-trans*. In the *s-cis* monomer, the methyl group in the α-position is in the *trans* position, relative to the carbonyl

dx.doi.org/10.1021/ct500507f | J. Chem. Theory Comput. XXXX, XXX, XXX−XXX

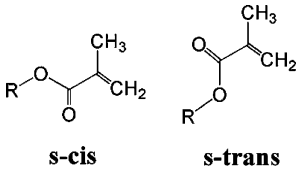

Figure 2. Representations of two different conformations of a methacrylate monomer: (left) *s-cis* and (right) *s-trans*. For MMA, R is the methyl group.

group, and in an *s-trans* monomer, the methyl group in the α-position is in the *cis* position, relative to the carbonyl group. Değirmenci et al. have reported a rotation barrier of ∼5 kcal mol^{-1} for the interconversion of these two conformers at the B3LYP/6-31+G(d) level of theory.[20] A previous study in our group also obtained a similar rotation barrier (∼6 kcal mol^{-1}) at the B3LYP/6-31G(d) level of theory.[12] We found that *s-trans* is 0.35 kcal mol^{-1} lower on the free-energy surface than *s-cis* using B3LYP/6-31G(2df,p), which is consistent with the result of Değirmenci et al.,[12] in which they found that the *s-trans* conformer is 0.26 kcal mol^{-1} more stable than the *s-cis* conformer. We have thus used *s-trans* monomer as the minimum on which to base the reported values. For the reactions reported below, in which the *s-cis* monomer was added, *s-trans* was still used as the reference point, since internal rotation is much faster than the bond-forming reaction. We mapped the potential energy surface for conversion of *s-trans* monomer to *s-cis* monomer via internal rotation, and at 298 K, the rate coefficient for internal rotation was calculated as 1.75 × 10^{8} s^{-1}. This is 6−7 orders of magnitude larger than the rate coefficient for the bond-forming reaction during propagation. In a PMMA chain, the carbonyl group and the α-methyl substituent in each unit can similarly be arranged in two conformations, just as in an isolated monomer. We denote a unit in which the methyl group of the α-substituent is in the *cis* position, relative to the carbonyl moiety, as "T", because it is the same pattern as a *s-trans* monomer; similarly, we use "C" to label a unit in which the methyl group of the α-substituent is in the *trans* position, relative to the carbonyl group, because it is in the same pattern as an *s-cis* monomer. This nomenclature is adopted below, and two examples of different monomer arrangements are shown in Figure 3. Since each MMA monomer can adopt either a "T" or "C"-type unit in a PMMA chain, it will generate 8 (2^3) different conformers for a trimer and 16 (2^4) different conformers for both the transition state and the tetrameric product. While earlier work on MMA polymerization has heavily investigated tacticity, which involves the relationship between two adjacent monomer units,[20] less emphasis has been placed on the preference within a monomer unit. Thus, in this study, we adopted syndiotactic structures that have been well-accepted as the dominant structure for MMA polymeric chains[45] and focused on the "T/C" motif of each repeating unit at the B3LYP/6-31G(2df,p) level of theory. We found that all conformers of a given species are very close in energy. For a given transition state, tetramer, and trimer, the range is less than 1.5 kcal mol^{-1}; detailed values are given in Table S1 in the Supporting Information. This result is not particularly surprising, given that limited intramolecular interactions of 1,3-units, given the small size of the methyl group on the ester moiety, are likely.

Next, we explored how significant the differences in E_a values would be if different conformations of the trimer, TS, and tetramer were used. To this end, a comparison of two different

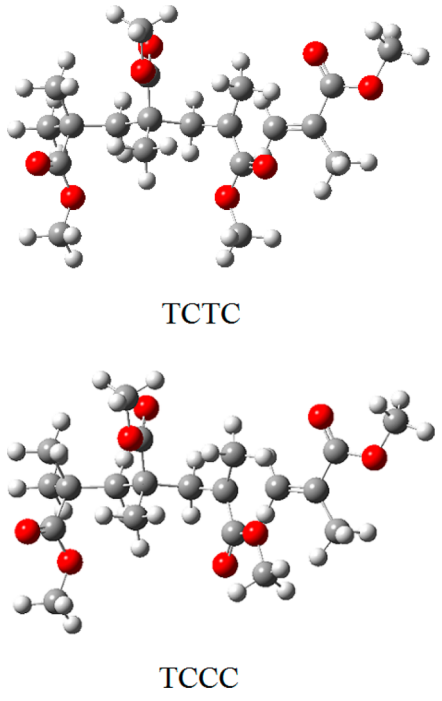

Figure 3. Representations of two different chain conformations of an MMA trimer-to-tetramer TS: (top panel) TCTC and (bottom panel) TCCC.

conformations is presented. However, all possible comparisons could be made with the information provided in the Supporting Information. At the B3LYP/6-31G(2df,p) level of theory, we identified that, among the 16 different conformations of the tetramer, the "TCCC" structure, which reads as an MMA tetramer consisting of "T", "C", "C", and "C" units from head to tail (radical site), is the lowest in energy. Similarly, "TCC-C" is the lowest-energy conformation of the TS and "TCC" is the lowest-energy conformation of the trimer. The structures adopted in the precedent work are identified as "TCTC" tetramer, "TCT-C" transition state, and "TCT" trimer, respectively, allowing the monomers to alternate. The comparison between these two particular sets of conformations is summarized in Table 1. It shows that every species (trimer, TS, and tetramer) where the "TCT" conformational sequence is present is slightly higher in energy than the corresponding "TCC" conformation. We then examined the predicted

Table 1. Comparison of Relative Free Energies, and Basis Set Superposition Error (BSSE)-Corrected Activation Energies Calculated from Two Sets of Different Conformers[a]

	ΔG (kcal mol^{-1})			
conformation	trimer	TS	tetramer	E_a (kcal mol^{-1})
TCCC	0.00	0.00	0.00	5.25
TCTC	0.90	0.51	0.50	5.15

[a]ΔG is the difference of free energy under standard conditions between an individual conformer and the lowest conformer found. Free energies used to identify the confomer geometry with the lowest energy were calculated at the B3LYP/6-31G(2df,p) level of theory. Free energies used for the calculation of activation energy were generated at the M06-2X/6-311+G(2df,p)//B3LYP/6-31G(2df,p) level of theory, with BSSE corrections on TS and tetramers.

dx.doi.org/10.1021/ct500507f | J. Chem. Theory Comput. XXXX, XXX, XXX−XXX

activation energies using these two sets of conformations. As shown in Table 1, the difference is as small as 0.1 kcal mol^{-1}. While it was possible in this work to exhaustively explore all possible conformations of this relatively low-molecular-weight monomer, this may not be the case for larger species. In addition, it is possible to take into account multiple pathways, accounting for the direction of approach of the monomer to the reacting radical. Ongoing work for related systems shows that taking these pathways into account has a more significant effect on calculated values of the pre-exponential factor than on the activation energy, although the pre-exponential factor can be reasonably well approximated by taking reaction path degeneracy into account. It is possible that there are large differences between the rate coefficients for different pathways, and thus, discrepancies between experimental and computational values may be due to this effect being discounted. However, it is important to stress that the computational cost of explicitly exploring all possible pathways is high. Overall, because the energy differences between "TCC" and "TCT" are minor, we carried out the benchmark study in section 3.2 using the "TCT+C" set ("T" monomer, "TCT" trimer, "TCT+C" TS, and "TCTC" tetramer) to allow direct comparison with previous work.

3.2. Effect of Basis Sets and Comparison of Different Density Fuunctional Theory (DFT) Methods. With the analysis of the different conformations complete, we proceeded to perform a comprehensive comparison of different levels of theory, comprised of different functionals and basis sets, using the "TCTC" configuration. The theoretical results were compared to experimental values for both the activation energy and heat of polymerization in order to identify an attractive level of theory to study the free-radical polymerization of methacrylate-type monomers. The activation energy of MMA homopropagation has been reported to be 5.37 kcal mol^{-1}, measured experimentally by PLP-SEC.[44] The heat of polymerization for MMA has been reported to be 13.5 kcal mol^{-1}.[46]

The activation energy and heat of polymerization predicted by various DFT methods using different basis sets are summarized in Figures 4 and 5, respectively. Although each DFT method gives distinct values, the trends in the values as the basis set is increased in size are independent of the DFT method. Although the trend is not precisely monotonic, the activation energy generally increases as the basis set size

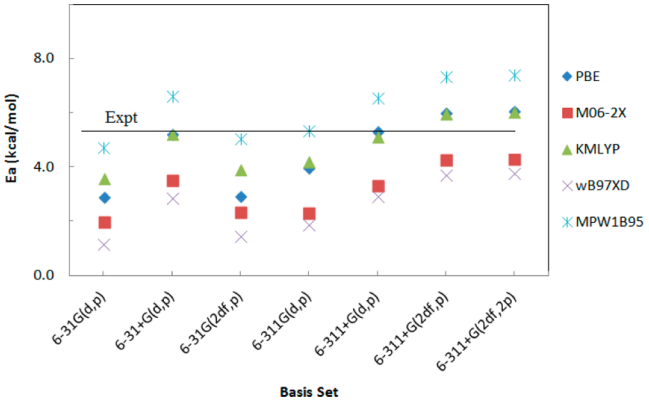

Figure 4. Comparison of activation energy of propagation of MMA calculated using different functionals in conjunction with different basis sets. All energy calculations are on the basis of optimized structures at the B3LYP/6-31G(2df,p) level of theory.

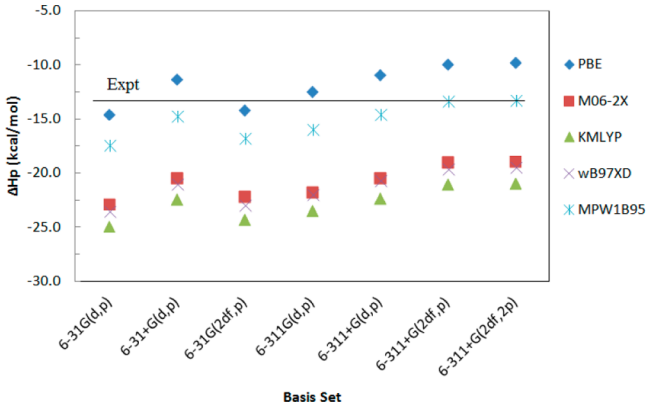

Figure 5. Comparison of heat of polymerization of MMA calculated using different functionals in conjunction with different basis sets. All energy calculations are on the basis of optimized structures at the B3LYP/6-31G(2df,p) level of theory.

increases, and the heat of polymerization decreases as the basis set size increases. These results indicate that using a smaller basis set has a tendency to overstabilize both the TS and tetramer, compared to a larger basis set. This is consistent with the well-established conclusion that BSSE is more significant on a smaller basis set.[47] Therefore, BSSE should be corrected in order to more accurately predict the activation energy and heat of polymerization for relatively small basis sets, which is done for a select DFT method below. Note that the use of diffuse functions in a basis set can effectively reduce BSSE, compared to a comparable basis set without diffuse functions, as shown in Figures 4 and 5. This is consistent with the recommendation of Lynch et al., who pointed out that the addition of diffuse functions is more important than increasing a double-ζ basis set to a triple-ζ basis set for calculating reaction barriers and reaction enthalpies.[40]

To demonstrate the effect of BSSE on calculated values of activation energy and heat of polymerization predicted for different basis sets, we specifically calculated E_a and ΔH_p values with BSSE included for M06-2X and compare them to uncorrected values in Figures 6 and 7, respectively. The comparisons also are very similar for other functionals. For 6-31G(d,p), the smallest basis set studied, the BSSE correction is large, i.e., as much as 3 kcal mol^{-1} for activation energy. Upon

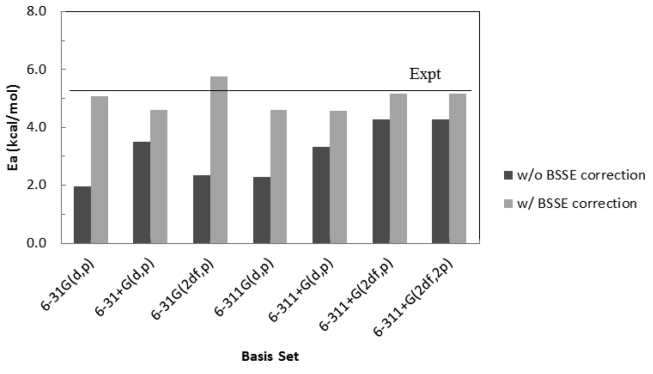

Figure 6. Comparison of uncorrected and BSSE-corrected activation energies of propagation for MMA calculated using the M06-2X functional in conjunction with different basis sets. All energy calculations are on the basis of optimized structures at the B3LYP/6-31G(2df,p) level of theory.

dx.doi.org/10.1021/ct500507f | J. Chem. Theory Comput. XXXX, XXX, XXX−XXX

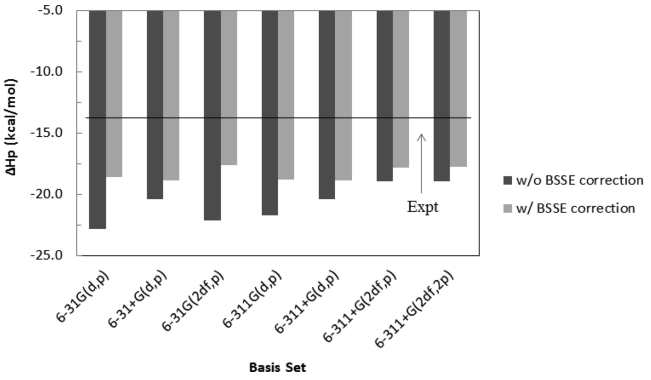

Figure 7. Comparison of uncorrected and BSSE-corrected heats of polymerization of MMA calculated using the M06-2X functional in conjunction with different basis sets. All energy calculations are on the basis of optimized structures at the B3LYP/6-31G(2df,p) level of theory.

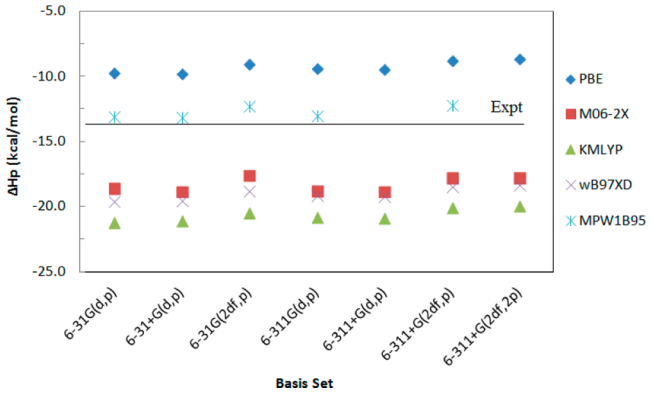

Figure 9. Comparison of BSSE-corrected heats of polymerization of MMA calculated using different functionals in conjunction with different basis sets. All energy calculations are on the basis of optimized structures at the B3LYP/6-31G(2df,p) level of theory.

the addition of diffuse functions, this difference is reduced to 1 kcal mol^{-1}. In contrast, when the basis set size is increased to a triple-ζ basis set without diffuse functions, the difference is 2 kcal mol^{-1}, in accordance with the observation of Lynch et al. Interestingly, the addition of d- and f-polarization functions to 6-31G(d,p) results in an even larger difference (3.4 kcal mol^{-1}). This result suggests that, for a double-ζ basis set, the addition of polarization functions would not effectively reduce the BSSE, but increase it. Similar conclusions can be drawn based on the ΔH_p values. Overall, we conclude that BSSE is crucial when a double-ζ basis set is used for calculation of the activation energy and heat of polymerization of MMA, and the addition of diffuse functions is more important than increasing to a triple-ζ basis set in order to reduce the BSSE.

The BSSE-corrected activation energy and heat of polymerization predicted by all DFT methods are summarized in Figures 8 and 9, respectively. Some MPW1B95 values were not obtained, because of a known SCF convergence issue with the B95 correlation functional.[48] Similar to the uncorrected values, the trend is the same for all methods with increasing basis set size. However, the BSSE-corrected values show a weak dependence on basis set, suggesting that small basis sets may

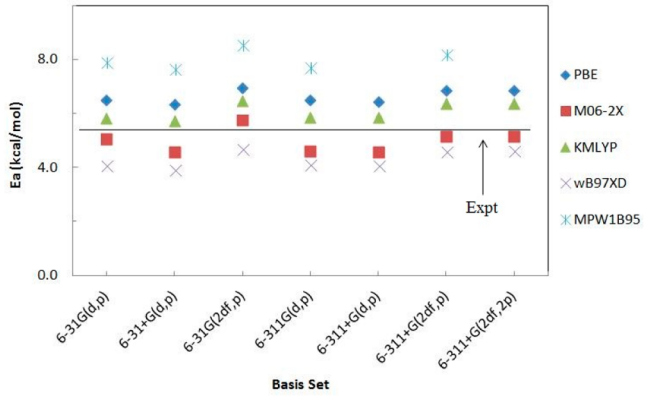

Figure 8. Comparison of BSSE-corrected activation energies of propagation of MMA calculated using different functionals in conjunction with different basis sets. All energy calculations are on the basis of optimized structures at the B3LYP/6-31G(2df,p) level of theory.

be serviceable, and it is more critical to select among different DFT functionals.

Figures 8 and 9 show that the calculated activation energy and heat of polymerization are sensitive to the choice of functional. Based on comparing to the experimental value of activation energy, M06-2X with the 6-311+G(2df,p) basis set provides the best agreement, while the slightly larger basis set, 6-311+G(2df,2p), gives almost the same value. Using the 6-311+G(2df,p) basis set to make further comparisons among functionals, the second best is wB97XD, which underestimates the activation energy by 0.77 kcal mol^{-1}. Note that M06-2X and wB97XD have been reported to reproduce the activation energy of poly(methyl acrylate) (PMA) chain propagation in the CBS limit reported by Yavuz and Çiftçioğlu.[23] KMLYP overestimates the experimental E_a value by 1.04 kcal mol^{-1}, and its error is comparable to that of wB97XD. KMLYP has been suggested to provide a viable choice as a cost-effective method for studying polymerization by Izgorodina and Coote in their previous work.[11] We discovered that it also performed reasonably well in this study. However, it is not as accurate as M06-2X, which was developed after the study by Izgorodina and Coote was published. PBE overestimates the activation energy by an even greater amount of 1.5 kcal mol^{-1}. Interestingly, in an earlier PMA study, PBE was shown to underestimate the activation energy by 1.5 kcal mol^{-1} in the CBS limit.[23] A noticeable difference in that work is that a monomer-to-dimer radical was adopted. MPW1B95 has also been shown to do well in predicting the activation energy of MA propagation,[23] but in the case of MMA propagation, it overestimates the activation energy by ~3 kcal mol^{-1}, showing poorer performance than the other functionals tested.

Our choice of functional to best reproduce the heat of polymerization is different from the one that best captures the activation energy. MPW1B95 gives the best estimate of ΔH_p, with an error of −1.3 kcal mol^{-1} compared to the experimental value. All other functionals that we tested produced errors that were at least ±4 kcal mol^{-1} from the experimental value. Both M06-2X and wB97XD overestimate it by a comparable amount (for M06-2X, 4.3 kcal mol^{-1}; for wB97XD, 4.8 kcal mol^{-1}). KMLYP deviated from the experimental value even more: −6.5 kcal mol^{-1}. In contrast, PBE underestimates the value by 4.8 kcal mol^{-1}. It is noted that PBE is the only functional that significantly underestimates the heat of polymerization, and it is the only one that contains no HF-exchange component. We

dx.doi.org/10.1021/ct500507f | J. Chem. Theory Comput. XXXX, XXX, XXX−XXX

then extended our investigation by doing a comparison of pure and hybrid functionals in three different functional families (BLYP[49,50] vs B3LYP, PBE vs PBE0,[51] and M06L[52] vs M06[37] vs M062X). All three families show that a hybrid functional gives a more exothermic heat of polymerization than its pure functional counterpart. Furthermore, the M06 family shows that a higher percentage of HF exchange has a tendency to give more exothermic values as well (see Table S2 in the Supporting Information). These results suggest that HF exchange may cause overestimation of the stability of the MMA tetramer radical, which leads to a more exothermic heat of reaction.

It has been established from previous studies on acrylonitrile and vinyl chloride that calculated values of E_a and ΔH_p are sensitive to the choice of electronic structure method. Furthermore, our work on MMA shows that they also are sensitive to the choice of basis set. Our test shows that the sensitivity to the basis set can be effectively removed by applying the BSSE corrections, which is consistent with a previous DFT study on reactions involving methyl radical addition to alkenes.[53] Unfortunately, no functionals tested in this work can simultaneously reproduce both E_a and ΔH_p within 2 kcal mol^{-1} of experimental values, which is a reasonable expectation for current DFT methods for similar systems. M06-2X performed well in the prediction of E_a, but overestimated ΔH_p by 4 kcal mol^{-1}; MPW1B95 performs very well for the prediction of ΔH_p, but overestimated E_a by 3 kcal mol^{-1}. In the context of kinetic modeling provided in the Introduction, E_a values will be the quantities where quantum chemistry values can play a critical role, as ΔH_p values are more widely available from experiments and may not be necessary in kinetic model formulation, since the polymerization reaction is highly irreversible under typical reaction conditions. Thus, M06-2X is recommended as the choice for calculating values for MMA-based (co)polymers. Early evaluations of this choice of method on other more bulky methacrylate monomers suggest that it also can be broadly applied.

3.3. ONIOM Calculations for Geometry Optimization. The geometries of all species from the ONIOM calculations were compared with their counterpart species from conventional DFT calculations described in section 3.2. Using conventional geometries as a reference, we found that the deviations between ONIOM and full QM geometries are small. A complete comparison of errors of ONIOM geometries, relative to conventional geometries, is provided in the Supporting Information. It is noted that even using the most aggressive partitioning (Partition 3), coupled with the smallest basis set (i.e., B3LYP/6-31G(d)) in the low-level layer, the mean absolute errors (MAEs) of TSs are negligible, which are 0.0018 Å for bond lengths, 0.10° for angles, and 0.15° for dihedrals in the low-level layer, and 0.0002 Å for bond lengths, 0.05° for angles, and 0.17° for dihedrals in the high-level layer. To evaluate if it is adequate to use ONIOM geometries to calculate E_a and ΔH_p, we then calculated them at the M06-2X/6-311+G(2df,p) level of theory using ONIOM geometries optimized with Partition 3 and the smallest basis set tested.

Both E_a and ΔH_p calculated from ONIOM geometries are shifted up by 0.7 kcal mol^{-1}, relative to their respective counterparts from conventional geometries, as indicated by Table 2. However, the results are still close to experimental values. Thus, results obtained from ONIOM geometries are comparable to those obtained from conventional geometries.

Table 2. Comparison of BSSE-Corrected Activation Energy and Heat of Polymerization Calculated from Conventional (Full QM) and ONIOM Geometries[a]

geom/energy	E_a (kcal mol^{-1})	ΔH_p (kcal mol^{-1})	$\Delta E_0^{\#}$ (kcal mol^{-1})	ΔZPE$^{\#}$ (kcal mol^{-1})
ONIOM	5.87	−17.07	4.06	0.90
conventional	5.15	−17.81	3.35	0.92
experiment	5.35	−13.79		

[a] E_a denotes activation energy, ΔH_p denotes heat of polymerization, $\Delta E_0^{\#}$ denotes difference of (ZPE) uncorrected electronic energies between TS and reactants, and ΔZPE$^{\#}$ denotes the difference in ZPE between TS and reactants. ONIOM refers to geometry optimization at the ONIOM(B3LYP/6-31G(2df,p):B3LYP/6-31G(d)) level of theory, and "conventional" refers to geometry optimization at the B3LYP/6-31G(2df,p) level of theory. All values were evaluated based on single-point calculations at the M06-2X/6-311+G(2df,p) level of theory.

4. CONCLUSION

In this work, we conducted a theoretical benchmark study on the kinetic and thermodynamic properties during methylmethacrylate (MMA) homopropagation, with the objective of determining a cost-effective approach to carry out kinetic studies of methacrylate radical polymerization.

We first performed a conformation study of MMA. The two conformers of MMA monomer, *s-cis* and *s-trans*, are very close in energy, and the species derived from them are distributed in a narrow energetic range of <1 kcal mol^{-1}. The benchmark test on different functionals coupled with basis sets of different sizes showed that both activation energy and heat of polymerization are highly sensitive to the basis set and the choice of functional. However, the dependence on the basis set can be systematically refined by the addition of diffuse functions and by applying basis set superposition error (BSSE) corrections. The BSSE-corrected results show that M06-2X/6-311+G(2df,p) predicts an activation energy in excellent agreement with experimental data but overestimates the heat of polymerization. The wB97XD functional provides results that are close to those from M06-2X with slightly larger errors in both activation energy and heat of polymerization. On the other hand, the MPW1B95 functional predicts an accurate heat of polymerization but significantly overestimates the activation energy. Given that the chief goal of this study was to estimate components of propagation rate coefficients, we recommend using the M06-2X functional in conjunction with the 6-311+G(2df,p) basis set for MMA and other methacrylate monomers. It is important to point out that the high level of theory, M062X/6-311+G(2df,p), is only for single-point calculations, which is viable for larger monomers containing more than three times the number of atoms as MMA, based on our experience, so we are able to extend the method to larger methacrylates as well.

We also investigated the feasibility of using ONIOM MO:MO calculations to speed up geometry optimizations as part of a cost-effective approach. Using ONIOM Partition 3 in Figure 1, which was the most aggressive and least expensive among all three partition schemes examined, we can still obtain accurate geometries and activation energy values in good agreement with results from the conventional DFT calculations. This suggests that the ONIOM method could effectively accelerate the study of bulkier methacrylate monomers without significant sacrifice of accuracy, as the high-level part is small and conserved across methacrylates.

dx.doi.org/10.1021/ct500507f | J. Chem. Theory Comput. XXXX, XXX, XXX−XXX

In summary, we propose here a cost-effective approach to calculate the activation energy of MMA homopropagation consisting of geometry optimization using ONIOM(B3LYP/6-31G(2df,p):B3LYP/6-31G(d)) + Partition 3 and subsequent energy calculation at the M06-2X/6-311+G(2df,p) level of theory with BSSE correction included. Currently, we are applying this protocol to other methacrylate monomers.

■ ASSOCIATED CONTENT

Supporting Information

Table of all conformers of methyl methacrylate (MMA) trimers, transition states (TSs), and tetramers. Table of heats of polymerization to allow comparison between different DFT methods. Tables of geometric comparisons between ONIOM and conventional calculations. Figures of TS showing the ONIOM partition scheme. This material is available free of charge via the Internet at http://pubs.acs.org.

■ AUTHOR INFORMATION

Corresponding Author

*E-mail: broadbelt@northwestern.edu.

Notes

The authors declare no competing financial interest.

■ ACKNOWLEDGMENTS

We are grateful for the financial support from the Dow Chemical Company and the computing resources from Northwestern University High Performance Computing.

■ REFERENCES

(1) Bauer, W., Jr., Methacrylic Acid and Derivatives. In *Ullmann's Encyclopedia of Industrial Chemistry*; Wiley−VCH Verlag GmbH & Co. KGaA: Weinheim, Germany, 2000; p 10.
(2) Odian, G. G. *Principles of Polymerization*, 4th Edition; Wiley−Interscience: Hoboken, NJ, 2004; pp 307−309.
(3) Beuermann, S.; Buback, M. *Prog. Polym. Sci.* **2002**, *27*, 191−254.
(4) Uetani, Y.; Inoue, H. Chemical amplification type positive resist composition. U.S. Patent 6,548,221, April 15, 2003.
(5) Kudo, T.; Padmanaban, M.; Dammel, R. R. Composition for coating over a photoresist pattern. U.S. Patent 7,595,141, Sept. 29, 2009.
(6) Asua, J. M.; Beuermann, S.; Buback, M.; Castignolles, P.; Charleux, B.; Gilbert, R. G.; Hutchinson, R. A.; Leiza, J. R.; Nikitin, A. N.; Vairon, J. P.; van Herk, A. M. *Macromol. Chem. Phys.* **2004**, *205*, 2151−2160.
(7) Junkers, T.; Barner-Kowollik, C. *J. Polym. Sci. Part A: Polym. Chem.* **2008**, *46*, 7585−7605.
(8) Fischer, H.; Radom, L. *Angew. Chem., Int. Ed.* **2001**, *40*, 1340−1371.
(9) Henry, D. J.; Parkinson, C. J.; Mayer, P. M.; Radom, L. *J. Phys. Chem. A* **2001**, *105*, 6750−6756.
(10) Coote, M. L. *Aust. J. Chem.* **2004**, *57*, 1125−1132.
(11) Izgorodina, E. I.; Coote, M. L. *Chem. Phys.* **2006**, *324*, 96−110.
(12) Yu, X. R.; Pfaendtner, J.; Broadbelt, L. J. *J. Phys. Chem. A* **2008**, *112*, 6772−6782.
(13) Yu, X. R.; Levine, S. E.; Broadbelt, L. J. *Macromolecules* **2008**, *41*, 8242−8251.
(14) Lin, C. Y.; Izgorodina, E. I.; Coote, M. L. *Macromolecules* **2010**, *43*, 553−560.
(15) Moscatelli, D.; Dossi, M.; Cavallotti, C.; Storti, G. *Macromol. Symp.* **2007**, *259*, 337−347.
(16) Moscatelli, D.; Dossi, M.; Cavallotti, C.; Storti, G. *J. Phys. Chem. A* **2011**, *115*, 52−62.
(17) Dossi, M.; Storti, G.; Moscatelli, D. *Polym. Eng. Sci.* **2011**, *51*, 2109−2114.
(18) Dossi, M.; Storti, G.; Moscatelli, D. *Macromol. Symp.* **2011**, *302*, 16−25.
(19) Degirmenci, I.; Avci, D.; Aviyente, V.; Van Cauter, K.; Van Speybroeck, V.; Waroquier, M. *Macromolecules* **2007**, *40*, 9590−9602.
(20) Degirmenci, I.; Aviyente, V.; Van Speybroeck, V.; Waroquier, M. *Macromolecules* **2009**, *42*, 3033−3041.
(21) Degirmenci, I.; Eren, S.; Aviyente, V.; De Sterck, B.; Hemelsoet, K.; Van Speybroeck, V.; Waroquier, M. *Macromolecules.* **2010**, *43*, 5602−5610.
(22) Miller, M. D.; Holder, A. J. *J. Phys. Chem. A* **2010**, *114*, 10988−10996.
(23) Yavuz, I.; Ciftcioglu, G. A. A. *Comput. Theor Chem.* **2011**, *978*, 88−97.
(24) Wang, L.; Broadbelt, L. J. *Macromolecules* **2009**, *42*, 8118−8128.
(25) Wang, L.; Broadbelt, L. J. *Macromolecules* **2009**, *42*, 7961−7968.
(26) Wang, L.; Broadbelt, L. J. *Macromol. Theory Simul.* **2011**, *20*, 54−64.
(27) Buback, M.; Kurz, C. H.; Schmaltz, C. *Macromol. Chem. Phys.* **1998**, *199*, 1721−1727.
(28) Vreven, T.; Byun, K. S.; Komaromi, I.; Dapprich, S.; Montgomery, J. A.; Morokuma, K.; Frisch, M. J. *J. Chem. Theory Comput.* **2006**, *2*, 815−826.
(29) Frisch, M. J.; Trucks, G. W.; Schlegel, H. B.; Scuseria, G. E.; Robb, M. A.; Cheeseman, J. R.; Scalmani, G.; Barone, V.; Mennucci, B.; Petersson, G. A.; Nakatsuji, H.; Caricato, M.; Li, X.; Hratchian, H. P.; Izmaylov, A. F.; Bloino, J.; Zheng, G.; Sonnenberg, J. L.; Hada, M.; Ehara, M.; Toyota, K.; Fukuda, R.; Hasegawa, J.; Ishida, M.; Nakajima, T.; Honda, Y.; Kitao, O.; Nakai, H.; Vreven, T.; Montgomery, J. A.; Peralta, J. E.; Ogliaro, F.; Bearpark, M.; Heyd, J. J.; Brothers, E.; Kudin, K. N.; Staroverov, V. N.; Kobayashi, R.; Normand, J.; Raghavachari, K.; Rendell, A.; Burant, J. C.; Iyengar, S. S.; Tomasi, J.; Cossi, M.; Rega, N.; Millam, J. M.; Klene, M.; Knox, J. E.; Cross, J. B.; Bakken, V.; Adamo, C.; Jaramillo, J.; Gomperts, R.; Stratmann, R. E.; Yazyev, O.; Austin, A. J.; Cammi, R.; Pomelli, C.; Ochterski, J. W.; Martin, R. L.; Morokuma, K.; Zakrzewski, V. G.; Voth, G. A.; Salvador, P.; Dannenberg, J. J.; Dapprich, S.; Daniels, A. D.; Farkas; Foresman, J. B.; Ortiz, J. V.; Cioslowski, J.; Fox, D. J. *Gaussian 09*, B.01; Gaussian, Inc.: Wallingford, CT, 2009.
(30) Becke, A. D. *J. Chem. Phys.* **1993**, *98*, 5648−5652.
(31) Curtiss, L. A.; Redfern, P. C.; Raghavachari, K. *J. Chem. Phys.* **2007**, *126*, 084108.
(32) Irikura, K. K., Appendix B. In *Computational Thermochemistry*; American Chemical Society: Washington, DC, 1998; Vol. *677*, pp 402−418.
(33) Hratchian, H. P.; Schlegel, H. B. *J. Chem. Phys.* **2004**, *120*, 9918−9924.
(34) Perdew, J. P.; Burke, K.; Ernzerhof, M. *Phys. Rev. Lett.* **1996**, *77*, 3865−3868.
(35) Kang, J. K.; Musgrave, C. B. *J. Chem. Phys.* **2001**, *115*, 11040−11051.
(36) Zhao, Y.; Truhlar, D. G. *J. Phys. Chem. A* **2004**, *108*, 6908−6918.
(37) Zhao, Y.; Truhlar, D. G. *Theor. Chem. Acc.* **2008**, *120*, 215−241.
(38) Chai, J. D.; Head-Gordon, M. *Phys. Chem. Chem. Phys.* **2008**, *10*, 6615−6620.
(39) Perdew, J. P.; Schmidt, K. *AIP Conf. Proc.* **2001**, *577*, 1−20.
(40) Lynch, B. J.; Zhao, Y.; Truhlar, D. G. *J. Phys. Chem. A* **2003**, *107*, 1384−1388.
(41) van Duijneveldt, F. B.; van Duijneveldt-van de Rijdt, J. G. C. M.; van Lenthe, J. H. *Chem. Rev.* **1994**, *94*, 1873−1885.
(42) Simon, S.; Duran, M.; Dannenberg, J. J. *J. Chem. Phys.* **1996**, *105*, 11024−11031.
(43) Yu, X. R.; Broadbelt, L. J. *Macromol. Theory Simul.* **2012**, *21*, 461−469.
(44) Beuermann, S.; Buback, M.; Davis, T. P.; Gilbert, R. G.; Hutchinson, R. A.; Olaj, O. F.; Russell, G. T.; Schweer, J.; van Herk, A. M. *Macromol. Chem. Phys.* **1997**, *198*, 1545−1560.
(45) Isobe, Y.; Yamada, K.; Nakano, T.; Okamoto, Y. *J. Polym. Sci., Part A—Polym. Chem.* **2000**, *38*, 4693−4703.

(46) Olabisi, O. *Handbook of Thermoplastics*. Marcel Dekker: New York, 1997; Vol. *41*, p 206.
(47) Grimme, S. *J. Comput. Chem.* **2004**, *25*, 1463−1473.
(48) Communication with Gaussian Technical Support.
(49) Becke, A. D. *Phys. Rev. A* **1988**, *38*, 3098−3100.
(50) Lee, C. T.; Yang, W. T.; Parr, R. G. *Phys. Rev. B* **1988**, *37*, 785−789.
(51) Adamo, C.; Barone, V. *J. Chem. Phys.* **1999**, *110*, 6158−6170.
(52) Zhao, Y.; Truhlar, D. G. *J. Chem. Phys.* **2006**, *125*, 194101.
(53) Arnaud, R.; Bugaud, N.; Vetere, V.; Barone, V. *J. Am. Chem. Soc.* **1998**, *120*, 5733−5740.